

N/Z effects on evaporation residue emission near fragmentation threshold

I.Lombardo^{1,3}, L. Acosta¹, C.Agodi¹, F.Amorini¹, A.Anzalone¹, L. Auditore⁵, I.Berceanu⁹, G.Cardella², S.Cavallaro^{1,4}, M.B.Chatterjee⁸, E.DeFilippo², G.Giuliani², E.Geraci^{2,4}, L.Grassi^{2,4}, J. Han¹, E.LaGuidara^{2,7}, G.Lanzalone^{1,3}, D.Loria⁵, C.Maiolino¹, T. Minniti⁵, A.Pagano², M.Papa², S.Pirrone², G.Politi^{2,4}, F.Porto^{1,4}, F.Rizzo^{1,4}, P.Russotto^{1,4}, S. Santoro⁵, A.Trifirò⁵, M.Trimarchi⁵, G.Verde², M. Vigilante⁹

¹INFN Laboratori Nazionali del Sud, Catania, Italy

²INFN, Sezione di Catania, Catania, Italy

³Facoltà di Ingegneria e Architettura, Università Kore di Enna, Enna, Italy

⁴Dipartimento di Fisica e Astronomia Università di Catania, Catania, Italy

⁵Dipartimento di Fisica, Università di Messina, Messina, Italy

⁶Dipartimento di Fisica, Università degli Studi Federico II, Napoli, Italy

⁷Centro Siciliano di Fisica Nucleare e Struttura della Materia, Catania, Italy

⁸Saha Institute of Nuclear Physics, Kolkata, India

⁹Institute for Physics and Nuclear Engineering, Bucharest, Romania

Abstract. We will discuss results concerning the fate of hot nuclear systems populated in $^{40,48}\text{Ca}+^{40,48}\text{Ca}$ reactions at 25 MeV/nucleon. Due to the complexity of events, we used the Chimera 4π device as detection system. By selecting central events of reaction, we found that the interplay between binary-like and evaporation residue emissions is strongly sensitive on the N/Z of the entrance channels. In particular, evaporation residue emission increases at increasing the neutron content of colliding system. By comparing our data with CoMD-II model calculations, we can extract information about the density depend part of Symmetry Potential in the Nuclear Equation of State at near-saturation densities.

1 Introduction

The fate of hot nuclear systems populated in heavy ion collisions at bombarding energies near 20 MeV/nucleon represents an interesting topic in nuclear physics [1]. In this energy regime, the reaction cross section for central collisions is distributed between evaporation residue emission (produced mainly by means of incomplete fusion mechanisms) and other more complex phenomena (such as damped binary-like emission or multi-fragment emission) [1,2]. This phenomenon has been attributed to a transition from a pure mean-field dynamics to more complex scenarios related to dynamical instabilities in the first phase of the collision, that lead to the destruction of the interacting system. In this energy regime, moreover, the density dependent part of symmetry energy could play a non negligible role in the evolution of reaction dynamics [3]. Actually, many dynamical models predict that the balance between evaporation residue emission and binary-like emission in this type of collisions can be an useful probe to determine the poorly known behaviour of the density dependent part of the symmetry energy in the Nuclear Equation of State [4-6].

To investigate this topic, we had the opportunity to perform a set of collisions involving medium mass nuclei ($^{40,48}\text{Ca}$ isotopes), used both as target or projectile, at 25 MeV/nucleon bombarding energies. In this way, we populated various nuclear systems differing for the neutron to proton ratio (N/Z) in the entrance channel. By selecting central events of reactions, we found that evaporation residues are emitted more likely in the very neutron rich system $^{48}\text{Ca}+^{48}\text{Ca}$, while in the neutron poor system $^{40}\text{Ca}+^{40}\text{Ca}$ binary-like and multi-fragment emission prevail. By comparing our experimental mass distributions with calculations performed with CoMD-II model [7], we can extract information about the stiffness degree of symmetry potential.

2 Experimental device

The experiment was performed at the INFN-Laboratori Nazionali del Sud Super Conducting Cyclotron facility in Catania (Italy). We accelerated beams of $^{40,48}\text{Ca}$ at 25 MeV/nucleon that impinged on self-supporting targets of ^{40}Ca (1.24 mg/cm^2) and ^{48}Ca (2.7 mg/cm^2). We used the Chimera (Charged Heavy Ions Mass and Energy Resolving Array) array as multi-detection device [8]. It is

performed by 1192 Si-CsI(Tl) telescopes, arranged in a cylindrical geometry, that cover 94% of the whole solid angle. The mean thickness of Si detectors is 300 μm . CsI(Tl) thicknesses are different, varying as a function of the polar angle. Further details about the functioning and performances of this device can be found in refs. [9,10]. In this experiment, we had also the opportunity to use a pulse shape analysis of silicon signal. In this way we will have the possibility to discriminate in charge those fragments stopped in the silicon detectors [11,12]. A typical energy-rise time matrix obtained for the $^{48}\text{Ca}+^{48}\text{Ca}$ experiment is shown in figure 1.

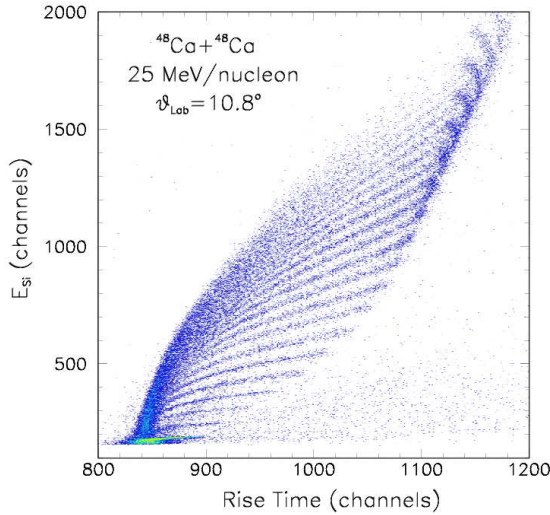


Fig. 1. Energy-rise time correlation for silicon signals of a well performing Chimera detector. The various branches correspond to different charges of fragments stopped in the silicon detector.

We analyzed only well detected events, i.e. events where the total detected charge was between 80% and 100% of the total charge in the entrance channels. Moreover we required to recover at least 70% of the initial linear momentum. Evaporation residues are identified in mass by means of time of flight technique. The experimental mass resolution achieved was $\Delta M/M \approx 5\%$ for evaporation residues having masses around 50 amu. Quasi-elastic reactions were removed during the data-taking by the chosen electronics trigger condition. It requires that at least 3 charged particles fire three silicon detectors.

3 Evaporation residue emission

Following the suggestion of ref. [13], we selected central collisions by means of a constraint on charged particle multiplicity. We focused moreover our attention on a class of events where the presence of a fast quasi-projectile nucleus is clearly recognized (massive transfer phenomena). To do this, we selected events where the second or the third largest fragment emitted had a velocity larger than 1.3 times the centre of mass velocity ($v_{\text{cm}} \approx 0.11c$) [14-16].

To characterize these events, we performed the mass-velocity correlation for the largest fragment emitted event

by event. The experimental results, obtained for $^{40}\text{Ca}+^{40}\text{Ca}$ ($N/Z=1.0$), $^{40}\text{Ca}+^{48}\text{Ca}$ ($N/Z=1.2$) and $^{48}\text{Ca}+^{48}\text{Ca}$ ($N/Z=1.4$) are shown in figure 2. Regardless their similarities, they show a quite different behaviour. In particular, for the most neutron rich system, $^{48}\text{Ca}+^{48}\text{Ca}$, an enhancement of evaporation residues (i.e. nuclei with masses ≈ 55 amu and velocity near $0.09c$) is seen. On the contrary, for the neutron poor system $^{40}\text{Ca}+^{40}\text{Ca}$, the most populated region of the scatter plot involves nuclei having masses near 30 amu, i.e. fragments emitted in binary-like, fusion-fission and fragmentation events. $^{40}\text{Ca}+^{48}\text{Ca}$ system, that is characterized by having an intermediate N/Z value ($=1.2$), shows an intermediate behaviour. It seems therefore that the neutron content of the total system has an important influence on the reaction dynamics; the larger is the neutron content of the entrance channel, the larger is the probability to observe an evaporation residue [14-16].

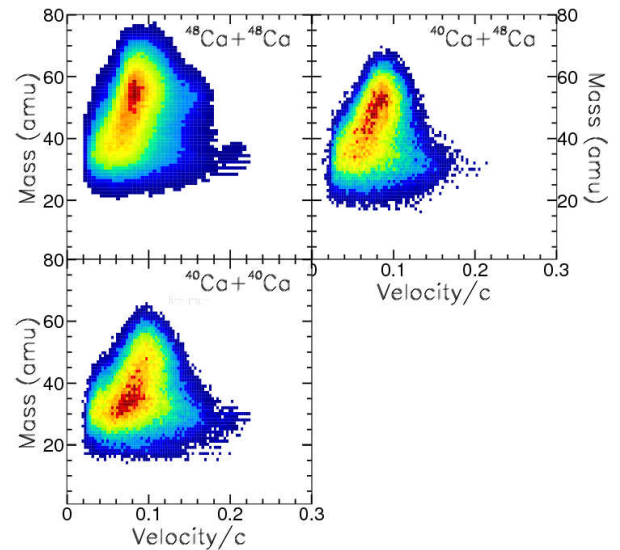


Fig. 2. Mass-velocity correlations for the largest fragment emitted in semi-central events of $^{48}\text{Ca}+^{48}\text{Ca}$ ($N/Z=1.4$), $^{40}\text{Ca}+^{48}\text{Ca}$ ($N/Z=1.2$) and $^{40}\text{Ca}+^{40}\text{Ca}$ ($N/Z=1.0$) reactions.

Mass spectra of the largest fragment emitted can be useful to extract the yield ratios of evaporation residue emission versus other mechanisms. We avoided small contaminations due to quasi-projectile and quasi-target emission by selecting only heavy fragments emitted in a range of velocity $0.04c < v < 0.15c$, i.e. centred on the v_{cm} velocity. Apart from effects due to the different total mass of the entrance channels (that can be reduced by normalizing the mass of fragment for the total mass of the system), mass spectra so obtained seem to be a superimposition of two Gaussian-like contributions [16] (see figure 3). The first one, peaked near 50-55 amu, can be related to evaporation residue emission, while the second one, peaked at lower values, can be attributed to binary-like and multi-fragmentation mechanisms.

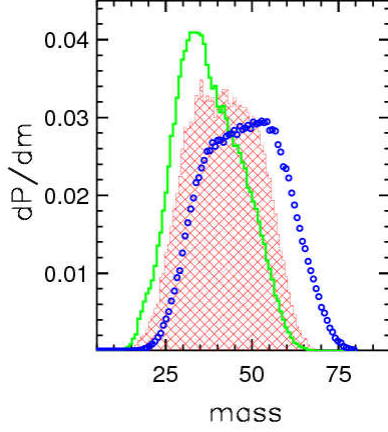


Fig. 3: Mass spectra of the largest fragment emitted in central events of $^{48}\text{Ca}+^{48}\text{Ca}$ (blue circles), $^{40}\text{Ca}+^{40}\text{Ca}$ (red grid area) and $^{40}\text{Ca}+^{48}\text{Ca}$ (green line) reactions.

We fitted these mass distributions by means of two Gaussian curves, and we were able to extract, from the fit procedure, the relative emission yield of evaporation residues, normalized to the whole number of central events selected as described previously in the text. In this way, a correlation between the N/Z of the entrance channel and the emission yield of evaporation residues can be traced, as shown in figure 4. In details, by increasing the N/Z of the entrance channel, the relative emission of evaporation residues (produced by means of incomplete fusion mechanisms) increases.

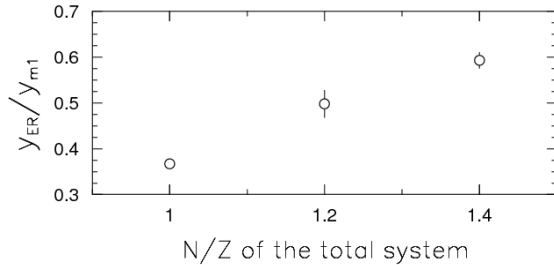


Fig. 4: Yields of evaporation residues emitted in central events of reactions, selected as described in the text. The emission yields have been extracted by means of a two Gaussian fit on the mass spectra of figure 3.

We had the opportunity to compare our experimental mass distributions with calculations performed with the dynamical model CoMD-II [17]. In particular, we compared the $\Delta M_{\text{nor}}=(m_1-m_2)/m_{\text{tot}}$ quantity, defined as the difference of the two largest fragments masses (that we call m_1 and m_2), normalized to the total mass of the entrance channel (m_{tot}). We found that the shape of the ΔM_{nor} distribution is sensitive to the various options adopted to describe the behaviour of the density dependent part of symmetry energy in the Nuclear Equation of State [17]. In particular, as it can be seen in figure 5, the best agreement between experimental data and CoMD-II model calculations (filtered by the GEMINI code [18] to take into account the statistical decay of excited fragments) is obtained when we choose a Stiff2 option for the symmetry potential, i.e. a linear dependence of the form factor on the nuclear density

achieved at the various steps of reaction. In figure 5 we show the case of $^{40}\text{Ca}+^{48}\text{Ca}$ reaction; similar results have been obtained for the other systems studied. Stiff1 option overestimate the region of $\Delta M_{\text{nor}}\approx 0.6$, corresponding to the emission of a big fragment (evaporation residue), while, at variance, the Soft option enhances the region of ΔM_{nor} spectrum near 0.1, i.e. there is a strong overestimation of binary-like and multi-fragmentation events. We checked moreover that the observed effect is a genuine dynamics effect; in fact the GEMINI stage does not modify the overall shape of ΔM_{nor} distribution (see figure 5c).

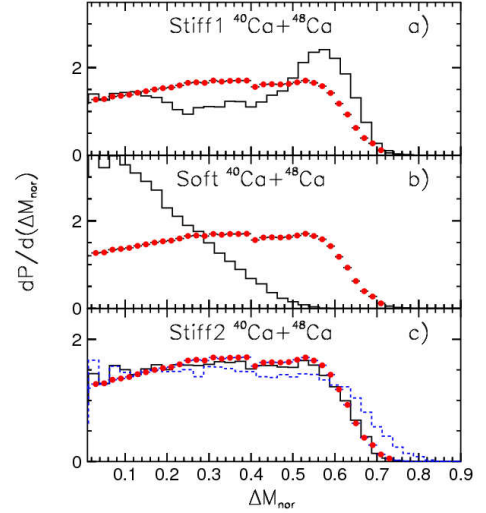


Fig. 5: Comparison of experimental ΔM_{nor} spectra (red dots) with CoMD-II model (GEMINI filtered) calculations (black histograms). The case of $^{40}\text{Ca}+^{48}\text{Ca}$ reactions is shown.

(a) Stiff1 option is used for the form factor of symmetry potential. (b) Soft option is used. Dashed histogram represent the result of CoMD-II calculation without the GEMINI stage.

4 Conclusions and Perspectives

We presented results concerning the emission of evaporation residues in nuclear collisions involving medium mass systems $^{40}\text{Ca}+^{40}\text{Ca}$, $^{40}\text{Ca}+^{48}\text{Ca}$ and $^{48}\text{Ca}+^{48}\text{Ca}$ at 25 MeV/nucleon bombarding energy, i.e. at the threshold of multi-fragment emission. By selecting central events of reactions, we found that the interplay between evaporation residue emission and other, more complex, phenomena (such as binary like and multi-fragment emission) is strongly dependent on the neutron content of the system. In particular, by increasing the N/Z of the total system, the probability of emitting an evaporation residue in incomplete fusion mechanisms is enhanced. By comparing our experimental mass distribution with CoMD-II dynamical model calculations, we observed that the symmetry potential of the nuclear equation of state plays a role on the interplay between the different reaction mechanisms observed. This finding opens the way for further investigations to be performed with radioactive beams having masses in the calcium region, but with exotic N/Z values (such as, for example, ^{34}Ar or ^{52}Ca). In this way, further details on the N/Z

dependence of evaporation residue emission at well above barrier collisions could be studied [19,20]. In this regard, we performed a transmission test of exotic beams having masses near 35 uma, produced with in-flight technique at the IFEB@LNS facility [21] at INFN-Laboratori Nazionali del Sud (the upgrade of the previous FRIBs separator [22]). Exotics beams were produced by fragmentation of an intense ^{36}Ar beam impinging on a ^9Be self supporting and cooled production target, 1.5mm thick. The produced nuclei are then selected in magnetic rigidity by means of the IFEB@LNS fragment separator line, and driven up to the Chimera experimental chamber. The tagging of the various beams is obtained by coupling a large surface micro-channel plate (working in transmission) with a double sided silicon strip detector (140 μm thick) set 13 m far from the micro-channel plate, along the beam line. A very good identification of the various nuclei composing the cocktail beam can be appreciated in figure 6. After some minor upgrades that should be operative at the end of 2011, we will be able to achieve intensities higher than 10^5 pps of ^{35}Ar and ^{37}K proton rich beams at 25 MeV/nucleon. It will be therefore interesting to investigate nuclear reactions involving this proton rich projectiles in order to enlarge our knowledge about the dynamics of evaporation residue emission at multi-fragmentation threshold.

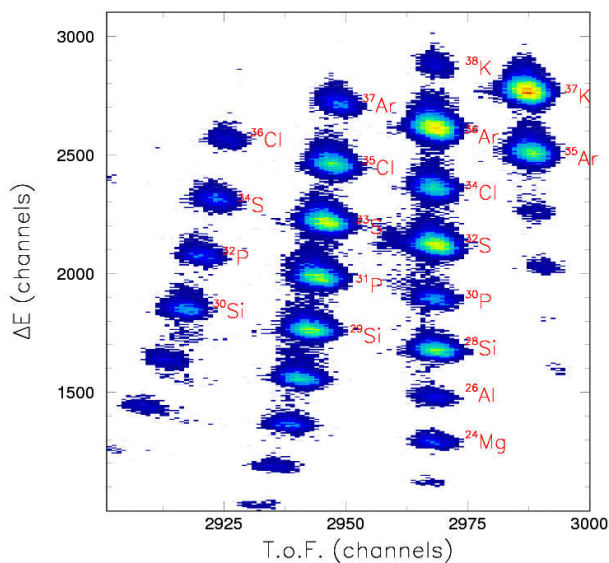


Fig. 6: ΔE -time of flight matrix obtained for a fragmentation cocktail beam at IFEB@LNS in-flight facility. A primary beam of ^{36}Ar at 42 MeV/nucleon impinged on a ^9Be target. The fragment separator magnetic fields were tuned to enhance the transmission of p-rich Ar isotopes. The ΔE -ToF identification matrix was obtained by using a tagging system based on MCP followed by a thin DSSSD [23].

References

1. D.A. Bromley, *Treatise on Heavy Ion Science*, Vol.2, Chapt. 3 (Plenum Press, NY, 1984)
2. P. Lautesse et al., *Eur. Phys. Jour. A* **27** 349 (2006)
3. V. Baran et al., *Phys. Rep.* **410**, 335 (2005)
4. M. Colonna et al., *Phys. Rev. C* **57** 1410 (1998)
5. L. Shvedov et al., *Phys. Rev. C* **81** 054605 (2010)
6. C. Rizzo et al., *Phys. Rev. C* **83** 014604 (2011)
7. M. Papa et al., *Phys. Rev. C* **68** 034606 (2003)
8. A. Pagano et al., *Nucl. Phys. A* **734** 504 (2004)
9. M. Alderighi et al., *Nucl. Instrum. Meth. Phys. Res. A* **489** 257 (2002)
10. N. Le Neindre et al., *Nucl. Instrum. Meth. Phys. Res. A* **490** 251 (2007)
11. M. Alderighi et al., *Nucl. Phys. A* **734** E88 (2004)
12. M. Alderighi et al., *IEEE Trans. Nucl. Sci.* **52** 1624 (2005)
13. C. Cavata et al., *Phys. Rev. C* **42** 1760 (1990)
14. F. Amorini et al., *Phys. Rev. Lett.* **102** 112701 (2009)
15. I. Lombardo et al., *Nucl. Phys. A* **834** 458 (2010)
16. I. Lombardo et al., *Acta Phys. Pol. B* **42** 701 (2011)
17. M. Papa, G. Giuliani, *Eur. Phys. Jour. A* **39** 117 (2009)
18. R.J. Charity, *Phys. Rev. C* **82** 014610 (2010)
19. G. Ademard et al., *Proceedings of the Fusion11 Conference*, EPJ Web of Conference (2011)
20. S. Pirrone et al., *Proceedings of the Fusion11 Conference*, EPJ Web of Conference (2011)
21. See the website: www.lns.infn.it
22. G. Raciti et al., *Nucl. Instr. Meth. Phys. Res. B* **266** 4632 (2008)
23. I. Lombardo et al., *Nucl. Phys. B (Proc. Suppl.)* **215** (2011) 272